Precise measurements of optical cavity dispersion and mirror coating properties via femtosecond combs

Michael J. Thorpe, R. Jason Jones, K. D. Moll, and Jun Ye

JILA, National Institute of Standards and Technology and University of Colorado
Boulder, Colorado 80309-0440
http://jilawww.colorado.edu/YeLabs/

Ramin Lalezari

Advanced Thin Films, 105 South Sunset St., Longmont, Colorado 80304

Abstract: We precisely determine the dispersion of an optical cavity over a large spectral bandwidth using a broadband optical comb generated by a femtosecond laser. This approach permits the effective characterization of the next generation of mirrors that will offer high reflectivity, minimal absorption/scattering loss, and well-defined dispersion characteristics. Such mirrors are essential for constructing passive, high-finesse cavities capable of storing and enhancing ultrashort pulses and for exploring novel intracavity-based experiments in atomic and molecular spectroscopy and extreme nonlinear optics. We characterize both zero and negative group-delay-dispersion mirrors and compare their performance against the targeted coating design. The high sensitivity of this approach is demonstrated with a precise determination of the group-delay dispersion of air inside a 40-cm long optical cavity, demonstrating an accuracy better than 1 fs^2.

OCIS codes: (320.7160) Ultrafast technology; (120.0120) Instrumentation, measurement, and metrology; (310.6860) Thin films, optical properties; (320.7100) Ultrafast measurements; (230.5750) Resonators; (230.4040) Mirrors

---

References and Links

1. T. Gherman, S. Kassi, A. Campargue, and D. Romanini, "Overtone spectroscopy in the blue region by cavity-enhanced absorption spectroscopy with a mode-locked femtosecond laser: application to acetylene," Chem. Phys. Lett. **383**, 353-358 (2004).
2. R. J. Jones, I. Thomann, and J. Ye, "Precision stabilization of femtosecond lasers to high-finesse optical cavities," Phys. Rev. A **69**, 051803 (2004).
3. R. J. Jones and J. Ye, "Femtosecond pulse amplification by coherent addition in a passive optical cavity," Opt. Lett. **27**, 1848-1850 (2002).
4. G. P. A. Malcolm, M. Ebrahimzadeh, and A. I. Ferguson, "Efficient Frequency-Conversion of Mode-Locked Diode-Pumped Lasers and Tunable All-Solid-State Laser Sources," IEEE J. Quantum Electron. **28**, 1172-1178 (1992).
5. R. J. Jones and J. Ye, "High-repetition rate, coherent femtosecond pulse amplification with an external passive optical cavity," Opt. Lett. **29**, 2812-2814 (2004).
6. J.-C. Diels and W. Rudolph, Ultrashort Laser Pulse Phenomena : Fundamentals, Techniques, and Applications on a Femtosecond Timescale (Academic Press, San Diego, 1996).
7. R. G. DeVoe, C. Fabre, K. Jungmann, J. Hoffnagle, and R. G. Brewer, "Precision Optical-Frequency-Difference Measurements," Phys. Rev. A **37**, 1802-1805 (1988).
8. C. J. Hood, H. J. Kimble, and J. Ye, "Characterization of high-finesse mirrors: Loss, phase shifts, and mode structure in an optical cavity," Phys. Rev. A **64**, 033804 (2001).
9. W. H. Knox, "Dispersion Measurements for Femtosecond-Pulse Generation and Applications," Appl. Phys. B **58**, 225-235 (1994)

10. J. Reichert, R. Holzwarth, T. Udem, and T. W. Hänsch, "Measuring the frequency of light with mode-locked lasers," Opt. Commun. **172**, 59-68 (1999).
11. J. C. Diels, R. J. Jones, and L. Arissian, in *Femtosecond Optical Frequency Comb: Principle, Operation, and Applications*, edited by J. Ye and S. T. Cundiff (Springer, 2005) pp. 333.
12. Advanced Thin Films provided all the custom-designed mirrors used in this work. Mentioning of manufacturer's name is for technical communications only and does not represent endorsement from NIST.
13. M.Born, E. Wolf, "Principles of Optics: Electromagnetic theory of propagation, interference and diffraction," 7th ed. (Cambridge University Press, 1999) pp. 101.

1. Introduction

We foresee an array of experiments stemming from precise coupling between a train of ultrashort laser pulses and a passive, high-finesse, and low dispersion optical cavity. The broad-bandwidth and high intracavity field generated in these "femtosecond enhancement cavities" will enable many unique experiments based on a single femtosecond laser. Such topics include wide-bandwidth atomic and molecular spectroscopy [1], the characterization of material nonlinearities, femtosecond laser stabilization [2], femtosecond pulse energy enhancement [3], the efficient generation of ultra-short light sources from nonlinear mixing [4], and they enable the development of novel, high-repetition rate sources in the extreme UV from high-harmonic generation due to the obtainable intracavity intensities ($>10^{13}$ W/cm^2). Previous work has shown that a clear understanding of the pulse-cavity interaction is important for effective coupling and coherently storing ultrashort pulses inside a high finesse, passive optical cavity [5]. For this area of research to advance further, it is now essential to obtain low-loss and dispersion-managed broad bandwidth mirrors. However, improved precision test and measurement capabilities are required to characterize these technologically advanced mirrors, with the aim of providing feedback to the design and manufacturing process.

While measurements on the dispersive properties of coatings are often carried out using standard white-light-interferometric techniques [6], more precise and definitive measurements of mirror dispersion properties come from cavity-based tests. The use of a cavity significantly enhances the dispersive phase measurement by allowing multiple interactions between light and the sample. Previous work used CW lasers to characterize the net cavity dispersion inside high-finesse, ultrastable optical cavities [7,8]. Inside a mode-locked laser, Knox *et al.* determined the net group-delay dispersion (GDD) inside a laser cavity by measuring the group delay at various spectral regions [9]. The present work exploits the interactions between ultrashort pulses and passive optical cavities, combining the advantages of cavity enhancement with the precision, resolution, and efficiency provided by a single, broad-bandwidth optical comb. In the approach we discuss in this paper, we measure the frequency detuning between the femtosecond optical frequency comb and the respective cavity modes across the entire mirror coating spectrum. The structured cavity transmission peaks indicate the spectral regions where the modes of the femtosecond comb coincide with the cavity modes. The frequency/wavelength dependence of the cavity free spectral range (FSR), which is directly related to the intracavity GDD, is then determined by measuring the change in the transmission peak positions as we vary the laser repetition frequency (f_{rep}) in a controlled manner. Dispersion measurements of this kind take only about one minute for data acquisition across the spectral window of interest. This measurement approach allows accurate characterization of the net cavity dispersion as well as any individual intracavity optical components including mirrors, transparent solids, and dilute gases.

2. Experimental layout and measurement principle

The mirrors under study are custom-designed to offer either zero or negative GDD, controlled within a ~ 100 nm spectral range centered at 800 nm. The absorption and scattering loss of the mirrors is limited to < 10^{-4}, while the reflectivity ranges from ~ 99.9% for input/output couplers to > 99.99% for high reflectors. We have designed and tested a three-mirror linear cavity geometry that allows the quick exchange of various mirrors. The experimental scheme

is shown in Fig. 1. The measurement cavity is located in an evacuated box to eliminate the effect of air dispersion when we measure the mirror coating. A femtosecond optical frequency comb ("fs comb") generated by a Kerr-lens mode-locked Ti:Sapphire laser with a spectrum spanning from 750 to 850nm is incident on the cavity. A narrow spectral region (~5 nm) of the light reflected from the cavity is detected with a grating and photodiode to derive a Pound-Drever-Hall frequency-locking error signal [2]. The average optical frequency of this part of the fs comb is then locked to the passive cavity by controlling the laser cavity length. This keeps the fs comb resonant with the cavity modes at the spectral region defined by the optical detection system, fixing the average optical frequency of this part of the comb at ν_l. However, f_{rep} of the Ti:Sapphire laser can still be scanned independently, due to the two degrees of freedom of the fs comb. In particular, mirror rotation [10] is used in the dispersive arm of the laser to produce a large scanning range for f_{rep} while introducing only small perturbations at ν_l. Stabilization of the fs comb to the passive cavity modes and scanning of f_{rep} are both achieved with piezoelectric actuators within the laser.
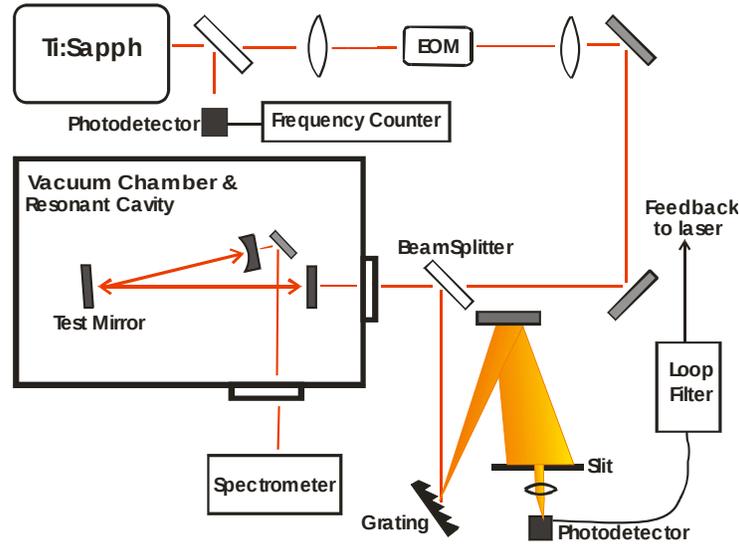

Fig. 1 Experimental scheme for intracavity dispersion measurement using a mode-locked femtosecond laser. The frequency locking error signal is obtained via frequency modulation generated by the electro-optic modulator (EOM), with the light detected in cavity reflection and after spectral selection. The cavity transmission spectrum is recorded to determine the cavity FSR.

Light transmitted from the cavity is analyzed via a spectrometer revealing the frequency positions of the fs comb that are resonate with the cavity. A fast photodiode is used to monitor f_{rep} of the laser and its frequency is counted continuously. The frequencies of the transmitted peaks are monitored with a spectrometer and recorded for a given value of f_{rep}. As f_{rep} is scanned, the position of the peak at ν_l does not change due to the servo control. However, the other transmission peaks will shift their positions as different parts of the fs comb are swept into resonance with the cavity modes at different wavelengths. We record many measurements of transmission peak positions and their corresponding values of f_{rep} until the transmission peaks have sampled through the entire mirror coating spectrum. The resulting data set maps transmission-peak positions, ν_t, to the corresponding values of f_{rep}. We will refer to this experimentally determined function as $F_{rep}(\nu_t,\nu_l)$, which is related to the intrinsic dispersion property of the cavity under measurement. The calculations in the following section demonstrate how the intra-cavity dispersion is obtained from $F_{rep}(\nu_t,\nu_l)$.

Measurements are performed by locking the fs comb to the cavity modes with f_{rep} slightly

offset from the cavity FSR at ν_l. Figure 2 shows the motivation behind such an arrangement. Due to the deliberately introduced difference between f_{rep} and the cavity FSR at ν_l, the modes of the fs comb quickly walk-off from resonance of the cavity modes away from ν_l. This results in the narrow transmission features shown in Fig. 2(a). The wavelength dependence of the cavity FSR (shown in Fig. 2(b) as a quadratic function around the center wavelength of the coating)
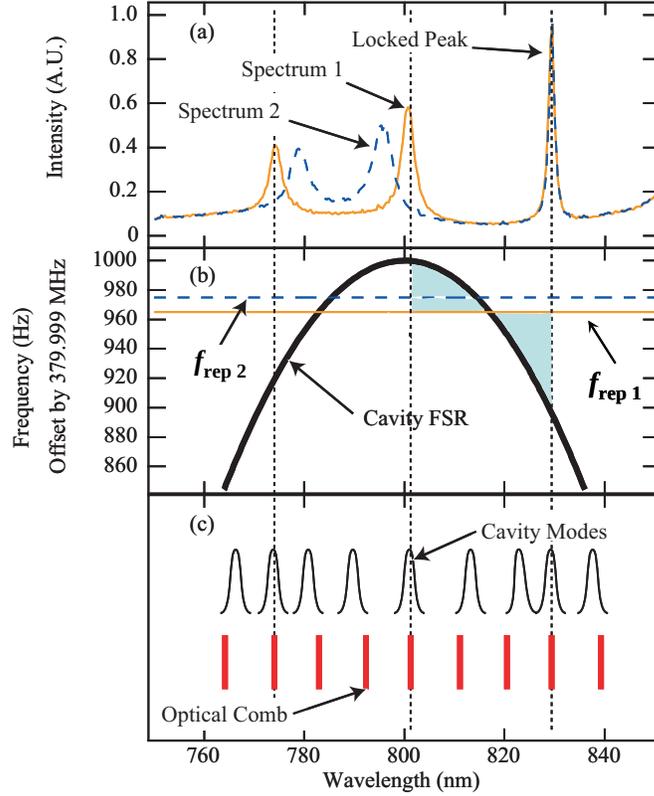

Fig. 2 Principle of intracavity dispersion measurement using a mode-locked laser. (a) Cavity transmission spectra obtained with two different values of the laser f_{rep}. The peak at 830 nm is the result of locking the average frequency of the selected comb to the cavity modes there. (b) The inverted parabola indicates the cavity FSR versus wavelength, due to the net cavity dispersion. Different settings of the laser f_{rep}, as shown by straight horizontal lines, allow different sections of cavity modes to become overlapped with the frequency comb, resulting in changes in the cavity transmission. The shaded area between f_{rep1} and the cavity FSR curve illustrates that the integral of the difference between these two curves over the frequency interval separating the two transmission peaks is zero (see Eq. (1)). (c) Cartoon showing the walk-off effect between the frequency comb and the non-uniformly spaced cavity modes. Near the locking frequency, the detuning between the laser f_{rep} and the cavity FSR cause the optical comb modes to walk-off from the cavity modes. Away from the locking region, the frequency-dependent cavity FSR causes the optical comb to realign with the cavity modes such that the mth comb component is once again resonant with the mth cavity mode.

brings the fs comb back into resonance such that the mth comb component once again overlaps with the mth cavity mode, as is the case in Fig. 2(c), where m is an integer and $m = 0$ corresponds to the central mode at ν_l. This is shown by the curve labeled as Spectrum 1 in Fig. 2 (a), which corresponds to the preset value of $f_{rep\ 1}$ shown in Fig. 2(b). When f_{rep} is changed, a new cavity transmission curve emerges (Spectrum 2 in Fig. 2(a)). We note that

Eqs. (1) and (2) presented in Section 3 that are used to analyze the measured function $F_{rep}(\nu_t,\nu_l)$ are only valid for the transmission peaks that correspond to the mth comb component overlapping with the mth cavity mode. Higher order transmission peaks that correspond to the $m \pm 1, 2, 3, \ldots$ comb component coinciding with the mth cavity mode are not included in this analysis. If we ignore these higher-order transmission peaks, then for the case of a monotonic change of FSR versus wavelength, there can exist only one transmission peak where the mth comb component will overlap with the mth cavity mode. For quadratic and higher order FSR curves this is not the case. As seen in Fig. 2, the curvature of the cavity FSR allows for two transmission peaks where the mth comb component overlaps the mth cavity mode.

3. Theoretical understanding

The picture of comb-cavity walk-off and the changing positions of the transmission peaks in Fig. 2(a) can be understood in terms of an integral containing the frequency-dependent FSR of the measurement cavity, FSR(ν) [11].

$$0 = \int_{\upsilon_t}^{\upsilon_l} [\frac{FSR(\upsilon)}{F_{rep}(\upsilon_t,\upsilon_l)} - 1] \ d\upsilon \ . \tag{1}$$

Equation (1) expresses the same idea in the previous section where the mth comb component rematches with the mth cavity mode after the initial walk-off from the locking region. By differentiating Eq. (1) with the variable ν_t, a simple relationship is reached between the frequency-dependent cavity FSR and the chosen values of laser f_{rep} :

$$FSR(\upsilon) = F_{rep}(\upsilon_t,\upsilon_l) + (\upsilon_t - \upsilon_l)\frac{d}{d\upsilon_t}F_{rep}(\upsilon_t,\upsilon_l) \ . \tag{2}$$

Equation (2) provides the motivation for our previously described measurement technique. With a given ν_l, and by measuring ν_t of the identified transmission peak and the corresponding $F_{rep}(\nu_t,\nu_l)$ across the entire spectrum, one can easily determine the frequency-dependent FSR(ν) of the cavity, from which the cavity GDD can be derived accordingly. The frequency dependent mode-spacing of the cavity can be written as FSR(ν) = c/[2L + c/2π(dφ/dν)] where φ(ν) is the frequency dependent round-trip phase shift introduced by reflections off the cavity mirrors or transmission through intracavity samples when they are present [3]. From the experimentally determined FSR, the total cavity GDD can be derived as GDD(ν) = d/dν [1/FSR(ν)].

In all measurements the FSR vs. f_{rep} data are fit by a polynomial that is used to determine the cavity GDD. In the case of the input coupler, high reflector, and dilute gas, the FSR vs. f_{rep} curve fit is performed globally due to its well-behaved functional form. In the case of the negative-GDD mirror, small sets of 10 data points (roughly 4 nm of data) are fit linearly and then patched together to form the data set shown in Fig. 3.

4. Measurements of low-loss, low-dispersion mirrors and intracavity gas samples

We first measured the GDD of a cavity containing three input couplers. Because the three mirrors are from the same coating run we assume and confirm that the single mirror GDD can be determined by dividing the total cavity GDD by the number of reflections in a single round-trip of the cavity. Once we have characterized the original mirror set we are able to exchange a cavity mirror with one of the test mirrors. Again we measure the total cavity GDD and then subtract off the contributions of the two original mirrors. This method could easily be improved upon by first constructing a two-mirror cavity and characterizing its dispersion. One could then construct a three-mirror cavity consisting of the original two mirrors and a sample mirror. The sample mirror dispersion is then found by subtracting the previously characterized two-mirror dispersion from the three-mirror cavity dispersion. In our
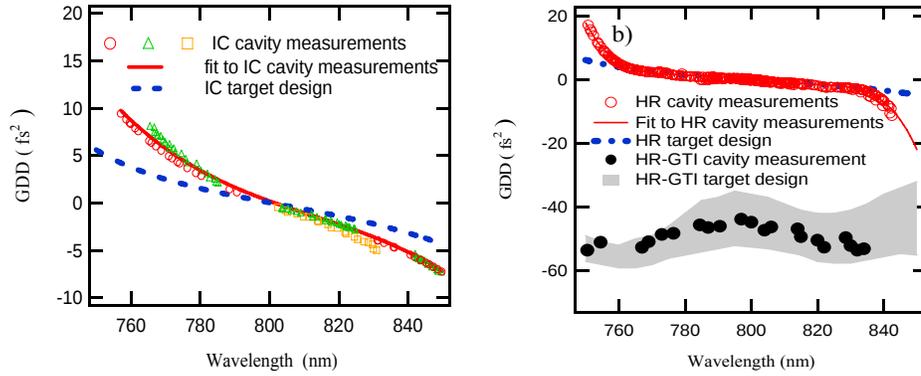
Fig. 3 (a) Cavity-based measurement of the GDD of zero-GDD mirrors used as an input coupler. Three independent measurements are shown. The design theory curve is shown as a dashed line. (b) Cavity-based measurement of the GDD of zero- (open circles) and negative-GDD (filled circles) high reflectors. Data from three independent measurements are shown for the zero-GDD mirror and a single data set is shown for the negative-GDD mirror. Also included are the design curves for both types of mirrors. Due to the sensitivity on layer thickness of the GTI structure, the range obtained from 20 theoretical curves corresponding to a 0.5% RMS variation in the layer thickness is shown. .

experiment, we found this to be unnecessary due to the high uniformity of input couplers used to construct the original cavity. Both theoretical analysis of the coating design (introduction of random error in the layer thickness) and tests where we exchanged one of the cavity mirrors with another from the same coating run showed that our input couplers varied in dispersion characteristics by no more than 1 fs^2 across the spectrum.

Figure 3(a) shows the measured GDD results (in open circles) for the zero-GDD input coupler mirror. The measured data are accompanied by a theoretical target design curve (dashed line) [12]. Figure 3(b) shows measurement results on two other mirror types; one is a zero-GDD high reflector, and the other is a negative-GDD high reflector, achieved with a double-Gires-Tournois interferometric (GTI) coating design on top of the highly reflective quarter-wave stacks. Measurements of both the input coupler and the high reflector show that even though the targeted dispersion characteristics of these mirrors are in good agreement with the measurements near the center wavelength of the coating, they deviate near the edge of the mirror bandwidth. Though, it should be noted that the measured dispersion is within 10 fs^2 of the targeted dispersion across the entire spectrum. Finally, since the theory of the GTI coating is so sensitive to random error in layer thickness, it is difficult to compare the GTI measurement to theory except to say that the measurement falls within the predicted band provided (shown as a gray band in Fig. 3(b)). With this technique, we are able to achieve a measurement repeatability of ~ 2 fs^2 for the input coupler and negative-GDD mirrors and < 1 fs^2 for high reflectors.

To rule out the possibility of systematic errors and to demonstrate the high sensitivity of this intracavity dispersion measurement technique, we filled our measurement cavity with 618 Torr of air at 20°C. We then measured the total cavity dispersion and subtracted off the dispersion contributions of the cavity mirrors measured under vacuum, leading to the net determination of the dispersion of air. Figure 4 shows measurement results plotted against the theoretical curve derived from the Sellmeier equation [13]. The measured group delay dispersion deviates from theory by less than 1 fs² across the entire spectrum supported by the mirror coating.
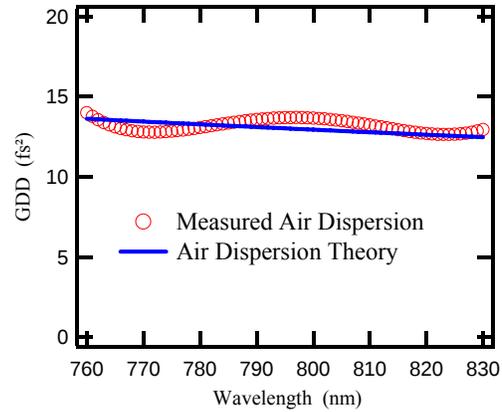
Fig. 4 Cavity-based measurement of the dispersion of air versus theory. The theory curve is derived using the Sellmeier equation for the air refractive index and multiplying it by the cavity length. This curve illustrates that the disagreement between the measurement method and theory across the entire spectrum is less than 1 fs².

5. Conclusion

The accurate information of the cavity GDD obtained with this technique has greatly enhanced our ability to compensate for the dispersion of intra-cavity elements, required for the development of "femtosecond enhancement cavities" that can maintain resonance with the broad spectrum of ultrashort pulses while still interacting with material necessary for useful experiments. For example, a combination of negative GDD mirrors and the appropriate level of air pressure in the cavity has been used to compensate an intracavity Bragg deflector [5]. Due to its high precision, this method will provide accurate feedback for the next generation of thin film coating designs.